SETSCI Conference Indexing System,
Volume 3 (2018), 947-953

ISAS 2018-Winter
2nd International Symposium on Innovative Approaches in Scientific Studies
November 30 – December 2, 2018, Samsun, Turkey

Investigation of Spectroscopic, Theoretical and Molecular Docking of vanillin thiosemicarbazone derivatives

Burak TÜZÜN[1*+], Sultan ERKAN[1]

[1]*Sivas Cumhuriyet University, Faculty of Science, Chemistry department, SİVAS*
[*]*Corresponding author: btuzun@cumhuriyet.edu.tr*
[+]*Speaker: btuzun@cumhuriyet.edu.tr*
Presentation/Paper Type: Oral/Full Text

Abstract- Thiosemicarbazones are biochemically interesting compounds which exert a wide range of biological activities, and, thanks to this property, are promising, as drugs, in the treatment of many diseases. Metal complexes may inhibit the protein synthesis because of interference in the cellular respiration. Cancer is leading cause of fatality in recent years and remained as a challenge for the world [2-3]. It is known that the study of the influence of the aromatic/aliphatic nature of the parent aldehyde/ketone on the overall hydrophobicity/hydrophilicity of the molecule, also modulated by the presence of hydrophilic fragments on the terminal amino group, can help improve our understanding of the relationship between the thiosemicarbazone molecular structure and the biological activity exerted. Optimized structures are calculated in B3lyp, HF and m062x, method 3-21g, 6-31g, sdd basis set.

The ^{1}H-NMR, ^{12}C-NMR, UV-VİS and IR spectra of these ligands will be examined by looking at their spectroscopic properties. At the same time, Molecular docking calculations are carried out between studied ligand and the 3DJU that is crystal structure of human BTG2 at DockingServer. Anti-cancer properties will be examined by the most optimized structures of ligands.

Keywords- vanillin thiosemicarbazone derivatives, Molecular docking, DFT, spectroscopy

1. Introduction

Cells require tight regulation of the intracellular redox balance and consequently of reactive oxygen species for proper redox signaling and maintenance of metal (e.g., of zinc and copper) homeostasis. In several diseases, including cancer, this balance is disturbed. Therefore, anticancer drugs targeting the redox systems have entered focus of interest. Many metal-containing compounds have been utilized throughout history to treat a wide variety of disorders. In medicinal chemistry —traditionally dominated by organic chemistry— metal complexes have gained favor as diagnostic tools and anticancer agents. Cancer is the second most frequent cause of death in the world. The discovery of antitumor activity of cisplatin began a search for other metal complexes with cytotoxic properties against cancer cells. Organo-metallic compounds have been used in medicine for centuries. Metal complexes play essential role in pharmaceutical industry and in agriculture. The metallo-elements present in trace quantities play vital roles at the molecular level in living system. The transition metal ions are responsible for proper functioning of different enzymes. Transition metals represent the D block element which includes groups 3 - 12 on the periodic table. Their d shells are in process of filling. The partially filled d orbital in transition metals impart interesting electronic properties that can act as suitable probes in the design of anticancer agents. This property of transition metals resulted in the foundation of coordination complexes.

2. Computational details

DFT calculation is the most popular method for the activity of molecules. In this study, we prepared the input files of the molecules studied by gaussian view 5.08 programs [5]. Calculations of studied molecules were performed with Gaussian IA32W-G09RevA.02 and Gaussian AS64L-G09RevD.01 programs [6-7]. Studied molecules were performed using the Hartree-Fock (HF) [8] and Becke, 3-parameter, Lee-Yang-Parr (B3LYP) [9-11] method with sdd, cep-4g, 3-21G, 6-31G, 6-31++G, lanl2dz basis set in gas and an aqueous phase. HOMO and LUMO are given information about activity of molecules. Chemical reactivity parameter of molecules is given to found a good corrosion inhibitor such as E_{HOMO}, E_{LUMO}, ΔE (HOMO-LUMO energy gap), electronegativity (χ), chemical potential (μ), chemical hardness (η), electrophilicity (ω), nucleophilicity (ε), global softness (σ) and proton affinity (PA) [12-16].

$$\mu = -\chi = \left(\frac{\partial E}{\partial N}\right)_{\upsilon(r)} \tag{1}$$

$$\eta = \frac{1}{2}\left(\frac{\partial^2 E}{\partial N^2}\right)_{\upsilon(r)} = \frac{1}{2}\left(\frac{\partial \mu}{\partial N}\right) \tag{2}$$

Ionization energy (I) and electron affinity (A) [17] of studied molecules are calculated with HOMO and LUMO energy that are interested Electronegativity, global softness and chemical hardness obtaining the following equations.

$$\chi = -\mu = \left(\frac{I + A}{2}\right) \tag{3}$$

$$\eta = \frac{I - A}{2} \tag{4}$$

As it is well known that global softness is defined as the inverse of the chemical hardness [18].

$$\sigma = 1/\eta \tag{5}$$

$$\chi = -\mu = \left(\frac{-E_{HOMO} - E_{LUMO}}{2}\right) \tag{6}$$

$$\eta = \left(\frac{E_{LUMO} - E_{HOMO}}{2}\right) \tag{7}$$

The global electrophilicity index (ω) that is investigated by Parr et al., is the inverse of nucleophilicity and are given in equality (8). Electrophilicity and nucleophilicity are used for the prediction organic and inorganic reaction mechanisms. Nucleophilicity (ε) is defined as the inverse of the electrophilicity in equations (9).

$$\omega = \mu^2/2\eta = \chi^2/2\eta \tag{8}$$

$$\varepsilon = 1/\omega \tag{9}$$

3. Result and discussion

vanillin thiosemicarbazone is investigated by Gaussian software program. This molecule is calculated at different basis set. The results obtained from these calculations are given in table 1. In figure 1, the studied molecules are optimized by the gaussian software. The figural representation of HOMO, LUMO and ESP are calculated by optimized structure.

Table 1. The calculated quantum chemical parameters with B3LYP method in gas phase (eV)

	E_{HOMO}	E_{LUMO}	I	A	ΔE	η	σ	χ	Pİ	ω	ε	dipol	Energy
2-(1H-indol-3-yldiazenyl)-4,5,6,7-tetrahydro-1,3benehiazole													
B3lyp/3-21g	-5,124	-1,239	5,124	1,239	3,885	1,943	0,515	3,181	-3,181	2,605	0,384	4,743	-28753,005
B3lyp/6-31g	-5,317	-1,430	5,317	1,430	3,887	1,943	0,515	3,374	-3,374	2,928	0,342	4,525	-28899,960
B3lyp/sdd	-5,382	-1,594	5,382	1,594	3,788	1,894	0,528	3,488	-3,488	3,212	0,311	4,232	-28902,753
Hf/3-21g	-8,022	2,522	8,022	-2,522	10,54	5,272	0,190	2,750	-2,750	0,717	1,395	5,577	-28625,266
HF/6-31g	-8,093	2,332	8,093	-2,332	10,42	5,213	0,192	2,880	-2,880	0,796	1,257	5,416	-28769,921
HF/sdd	-8,181	2,119	8,181	-2,119	10,30	5,150	0,194	3,031	-3,031	0,892	1,121	5,127	-28772,397
M062x/3-21g	-6,631	-0,276	6,631	0,276	6,355	3,177	0,315	3,454	-3,454	1,877	0,533	4,651	-28744,169
M062x/6-31g	-6,816	-0,442	6,816	0,442	6,374	3,187	0,314	3,629	-3,629	2,066	0,484	4,429	-28891,478
M062x/sdd	-6,889	-0,625	6,889	0,625	6,264	3,132	0,319	3,757	-3,757	2,253	0,444	4,190	-28894,606

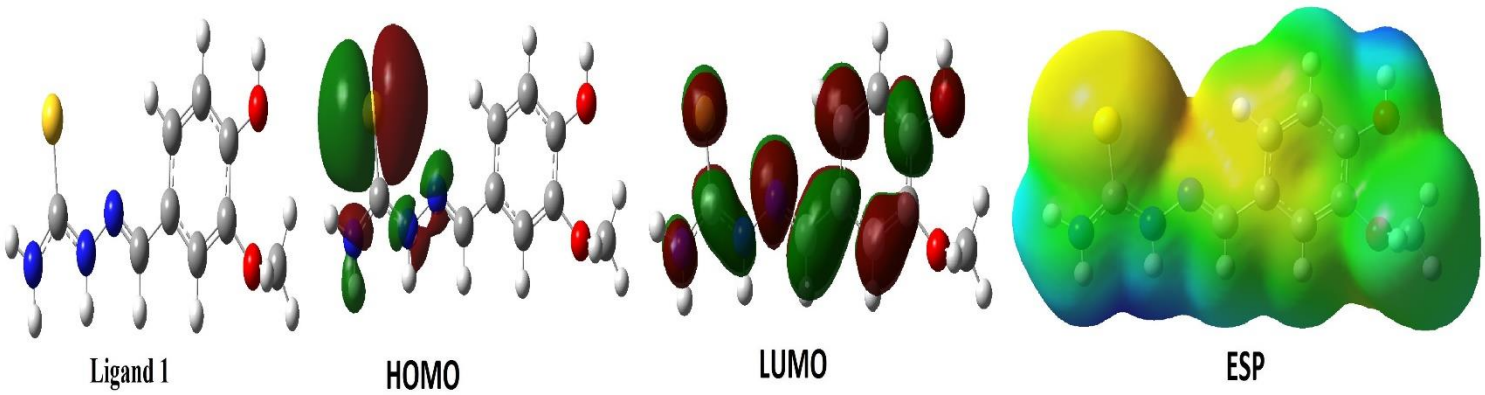


Figure 1. The structure and schematic representation of ligands

IR spectrum of studied molecule are calculated in gas phase at hf/6-31g basis set. IR spectrum of mentioned molecules is significant in determination of functional groups of molecules. These spectrums are represented in figure2.

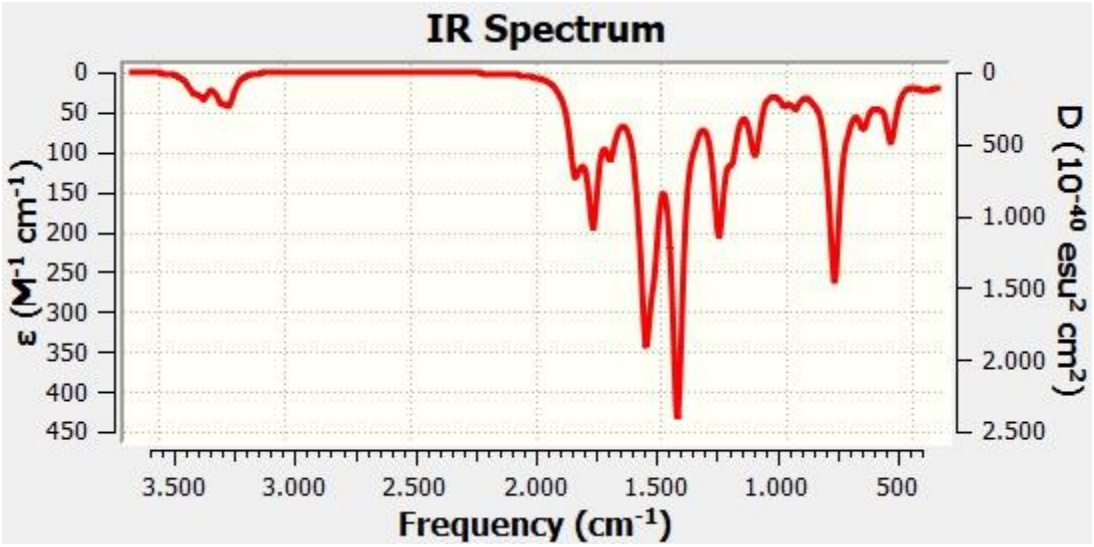


Figure 2. IR spectrum of this molecule

The ^{1}H and ^{13}C NMR chemical shifts of the molecule studied is given in Figure 3. NMR spectrum of ^{13}C NMR chemical shifts in the upper figure and ^{1}H NMR chemical shifts in the below figure are given in figure 3.

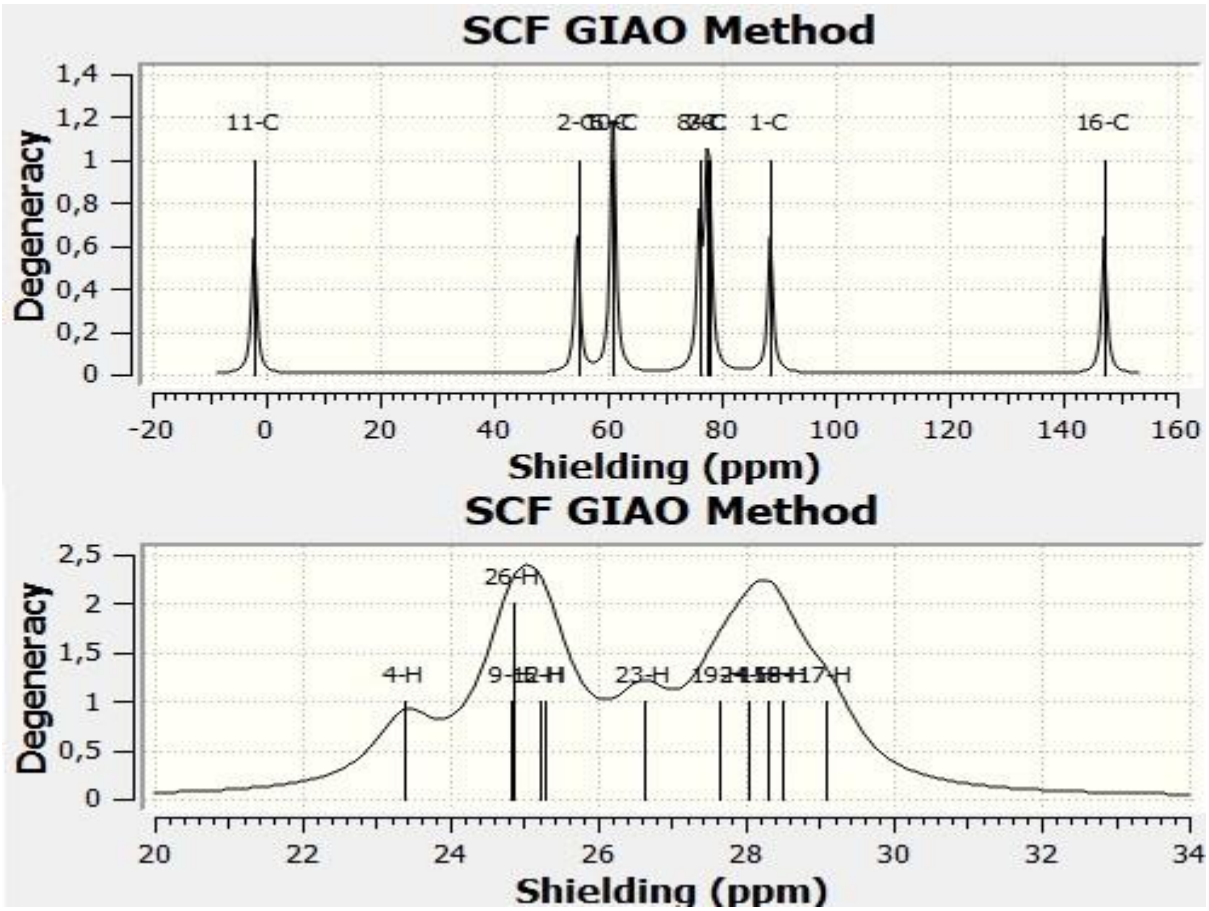


Figure 3. ^{1}H (below) and ^{13}C (upper) NMR chemical shifts of studied ligand

UV-VIS spectrum of studied molecules and complexes are calculated at same level basis set. UV-VIS spectrum of two ligands are very similar spectrums that have two main band. Each peak take place from many electronic transitions. Their wavelengths are 208 and 295 nm that have higher than 35000 Epsilon.

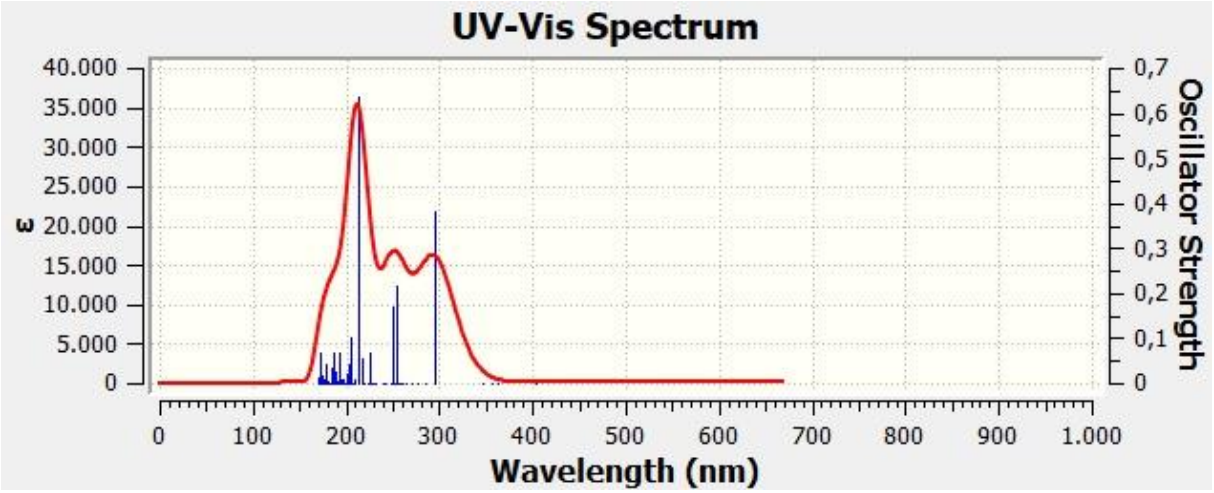


Figure 4. calculated UV-VIS spectra of ligand

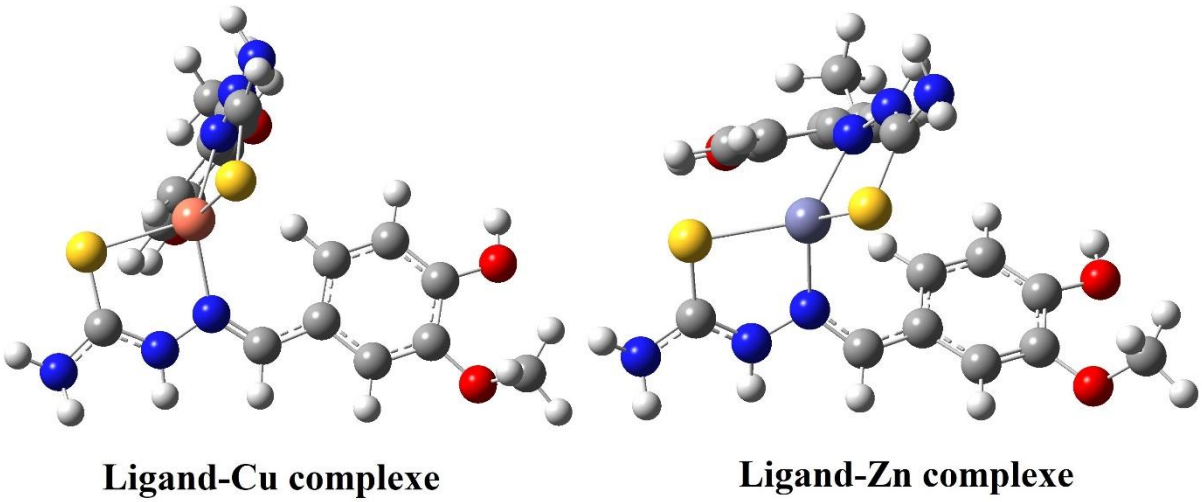


Figure 5. optimized structure of metal complexe

In this work, ligands were interacted with zinc and copper atoms. thermodynamic energy values of the complexes of ligands formed with zinc and copper atoms are given in table 2. As a result of these interactions, the resulting complexes are distorted square planes. When these complexes are observed, the Gibbs Free Energy values of these complexes appear to be formed spontaneously in table 2.

Table 2. ΔG of the complexes formed with metal atoms of ligands

$\Delta G_{Zn\text{-complexe}}$	-299,21641
$\Delta G_{Cu\text{-complexe}}$	-303,86799

Studied molecule are calculated at DockingServer. Numerical values of studied molecule are given table 6. The protein is obtained from Protein Data Bank by ID 3DJU, the molecular docking calculations are performed on DockingServer for virtual placement of small molecules into macromolecular receptors and developed for making related accounts.

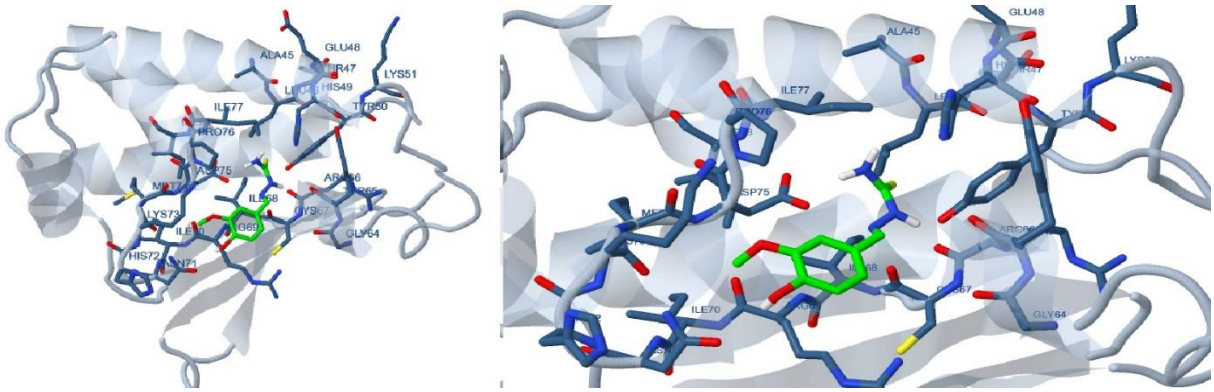


Figure 6. studied molecule interaction with protein 3DJU

Table 4. Molecular Docking energy data for studied molecule

	Ligand
Est. Free Energy of Binding, kcal/mol	-3,86
Est. Inhibition Constant, Ki, uM	1,49
vdW + Hbond + desolv Energy, kcal/mol	-5,95
Electrostatic Energy, kcal/mol	-0,16
Total Intermolec. Energy, kcal/mol	-6,12
Frequency	%10
Interact. Surface	526,282

References

1) isceglie, F., Tavone, M., Mussi, F., Azzoni, S., Montalbano, S., Franzoni, S., Pelosi, G. Effects of polar substituents on the biological activity of thiosemicarbazone metal complexes. Journal of inorganic biochemistry, 179 (2018) 60-70.
2) Sarigül M., Deveci P., Köse M., Arslan U., Dagi H.T., Kurtoglu M., journal of molecular structure 2015, 1096, 64-73
3) Williams N.H., Takasaki B., Wall M., J. Chin. Acc. Chem. Res. 1999, 32, 485-493
4) Surendra M.S., Umamaheswara B., Krishna V., J. Saudi Chem. Soc. 2017, 21, 291-299
5) Dennington R.D., Keith T.A., Millam J.M., GaussView 5.0, 2009. Wallingford CT.
6) Frisch M.J., Trucks G.W., Schlegel H.B., Scuseria G.E., Robb M.A., Cheseman J.R., Scalmani G., Barone V., Mennucci B., Petersson G.A., Nakatsuji H., Caricato H., Li X., Hratchian H.P., Izmaylov A.F., Bloino J., Zheng G., Sonnerberg J.L., Hada M., Ehara
7) M., Toyota K., Fukuda R., Hasegawa J., Ishida M., Nakajima T., Honda Y., Kitao O., Nakai H., Vreven T., Montgomery J.A., Peralta J.E., Ogliaro F., Bearpark M., Heyd J.J., Brothers E., Kudin K.N., Staroverov V.N., Kobayashi R., Normand J., Raghavachari K., Rendell A., Burant J.C., Iyengar S.S., Tomasi J., Cossi M., Nega R., Millam J.M., Klene M., Knox J.E., Cross J.B., Bakken V., Adamo C., Jaramillo J., Gomperts R., Stratmann R.E., Yazyev O., Austin A.J., Cammi R., Pomelli C., Ochterski

8) J.W., Martin R.L., Morokuma K., Zakrzewski V.G., Voth G.A., Salvador P., Dannenberg J.J., Daprich S., Daniels A.D., Farkas A., Foreaman J.B., Ortiz JV, Cioslowski J, Fox DJ. Gaussian 09, Revision D.01, Gaussian, Inc., Wallingford CT, 2009.
9) Frisch M.J., Trucks G.W., Schlegel H.B., Scuseria G.E., Robb M.A., Cheseman J.R., Scalmani G., Barone V., Mennucci B., Petersson G.A., Nakatsuji H., Caricato H., Li X., Hratchian H.P., Izmaylov A.F., Bloino J., Zheng G., Sonnerberg J.L., Hada M., Ehara M., Toyota K., Fukuda R., Hasegawa J., Ishida M., Nakajima T., Honda Y., Kitao O., Nakai H., Vreven T., Montgomery J.A., Peralta J.E., Ogliaro F., Bearpark M., Heyd J.J., Brothers E., Kudin K.N., Staroverov V.N., Kobayashi R., Normand J., Raghavachari K., Rendell A., Burant J.C., Iyengar S.S., Tomasi J., Cossi M., Nega R., Millam J.M., Klene M., Knox J.E., Cross J.B., Bakken V., Adamo C., Jaramillo J., Gomperts R., Stratmann R.E., Yazyev O., Austin A.J., Cammi R., Pomelli C., Ochterski J.W., Martin R.L., Morokuma K., Zakrzewski V.G., Voth G.A., Salvador P., Dannenberg J.J., Daprich S., Daniels A.D., Farkas A., Foreaman J.B., Ortiz JV, Cioslowski J, Fox DJ., Gaussian 09, Revision A.02, Gaussian, Inc., Wallingford CT, 2009
10) Becke A.D., A new mixing of Hatree-Fock and local density-functional theories, J.Chem. Phys. 98 (1993) 1372- 1377.
11) Wiberg K.B.. Basis set effects on calculated geometries: 6-311++G** vs. aug-cc-pVDZ. J. Comput. Chem. 25 (2004) 1342–1346.
12) Beck A.D., Density-functional thermochemistry III. the role of exact, Exchange the journal of chemical physics 98 (1993) 5648-5652.
13) Lee C., Yang W., Parr R.G., Development of the Colle-Savletti correlation-energy formula into a functional of the electron density, Physical Review 37 (1988) 785-789.
14) Tüzün B., Selectivity of Salicylaldoxime and its Derivatives, Journal of New Results in Science 3-5 (2014) 67-85
15) Tüzün B., Theoretical evalution of six indazole derivatives as corrosion inhibitors based on dft, Turkish computational and theoretical chemistry, 2-1 (2018) 12-22
16) Kaya S., Tüzün B., Kaya C., Conceptual Density Functional Theoretical Investigation of the Corrosion Inhibition Efficiencies of Some Molecules Containing Mercapto (-SH) Group. Current Physical Chemistry 7-2 (2017) 147-153
17) Hepokur C., Günsel A., Yarasir M.N., Bilgiçli A.T., Tüzün B., Tüzün G., Yaylim I., Novel type ketone-substituted metallophthalocyanines: synthesis, spectral, structural, computational and anticancer studies, RSC Advances 89 (2017) 56296-56305
18) Kaya S., Tüzün B., Kaya C. Conceptual Density Functional Theoretical Investigation of the Corrosion Inhibition Efficiencies of Some Molecules Containing Mercapto (-SH) Group. Current Physical Chemistry, 7(2) (2017) 147-153.
19) Madkour L.H., Elshamy I.H. Experimental and computational studies on the inhibition performances of benzimidazole and its derivatives for the corrosion of copper in nitric acid. Int. J. Ind. Chem. 7 (2016) 195–221.
20) Pearson RG. Chemical hardness: applications from molecules to solids. Germany: Wiley-VCH: Weinheim; 1997.